

LRFD FLEXURAL PROVISIONS FOR PSC BRIDGE GIRDERS STRENGTHENED WITH CFRP LAMINATES

Sherif El-Tawil, PhD, PE

Assistant Professor, Dept. of Civil and Env. Engineering, University of Central Florida, Orlando, FL 32816-2450, Tel.: (407) 823-3743, Fax: (407) 823-3315 Email: el-tawil@mail.ucf.edu

Ayman M. Okeil, PhD

Visiting Assist. Prof., Dept. of Civil and Env. Engineering, University of Central Florida, Orlando, FL 32816-2450 Tel.: (407) 823-3779, Fax: (407) 823-3315 Email: aokeil@maha.engr.ucf.edu

ABSTRACT

The behavior and design of pre-stressed concrete (PSC) bridge girders flexurally strengthened with carbon fiber reinforced polymer (CFRP) laminates are discussed. A fiber section model that accounts for inelastic material behavior as well as the construction sequence including transfer, composite action between the cast in place deck and girder, and bonding of CFRP laminates is developed. The model is verified and is then used to conduct thousands of Monte Carlo simulations of a number of bridges designed according to the 1998 AASHTO LRFD. The bridge designs address a broad range of design parameters including span length, ratio of dead load to live load, and amount of CFRP strengthening. The numerical simulations are used to develop cross-sectional resistance models from which the flexural reliability of the designed bridges is calculated using the first order reliability method. An equation for the flexural strength reduction factor for PSC bridge girders strengthened with CFRP laminates is proposed.

KEYWORDS

Bridge, prestressed, rehabilitation, CFRP, reliability, Monte Carlo simulation, FORM.

INTRODUCTION

Concrete bridge girders become structurally deficient for several reasons including corrosion of reinforcing bars or prestressing strands and changes in load requirements. In general, it is more economical to strengthen deficient girders than to replace the entire bridge. Carbon fiber reinforced polymer (CFRP) laminates are particularly suited for this purpose. The CFRP laminates are externally bonded to the girders and provide additional tensile resistance, which can improve flexural and shear strength. This rehabilitation technique has gained popularity in recent years as bridge engineers have become more familiar with the appealing attributes of FRP which include light weight, high strength and stiffness, resistance to corrosion, and good fatigue characteristics. Prominent examples of the use of this technology in bridge rehabilitation can be found in a report published by ACI ¹.

Many experimental and analytical studies have been conducted to explore both the short- and long-term behavior of *reinforced concrete* (RC) beams flexurally strengthened with CFRP laminates ³⁻⁵. The research conducted to date has focused on the effect of CFRP rehabilitation on the stiffness, strength, fatigue, ductility, mode of failure, and reliability of reinforced concrete girders strengthened with CFRP laminates. Research in this field has matured to the extent that code committees are starting to crystallize available knowledge into code provisions ⁶.

In contrast to the abundant information on RC girders strengthened with CFRP laminates, data on the behavior of PSC beams strengthened with CFRP is rather limited. This paper presents the results of research conducted at the University of Central Florida on the behavior and design of PSC girders flexurally strengthened with CFRP laminates. The focus of the paper is on the flexural strength reduction factor, ϕ , that is needed for the development of LRFD

provisions for PSC girders strengthened with CFRP laminates. The strength reduction factor is calibrated using a reliability-based technique that accounts for the randomness in important design variables and that ensures that a certain *Probability of Failure, P_f* , is attained. The research presented herein focuses exclusively on *flexural* behavior and assumes that other modes of failure such as shear failure, laminate peel-off, concrete cover delamination, and bond failure between laminates and concrete do not control behavior. Such modes of failure can be precluded by additional strengthening or through special detailing ⁴.

To achieve the goals set for this research, the following tasks are undertaken: 1) A fiber section model that accounts for material inelasticity and construction sequence is developed for conducting bridge cross-section design and analysis. 2) A number of realistic PSC bridge designs are generated, i.e. a design space is created. The designs have different spans and are based on current code provisions in AASHTO-LRFD ⁷. Each of the bridge designs is assumed to have lost a variable number of prestressing strands and is then strengthened back to its original design strength through externally bonded CFRP laminates. 3) Monte Carlo simulations are performed on each of the designed and rehabilitated bridges and the resulting data sets are used to develop resistance models for cross-sectional flexural strength. 4) The developed resistance models are used to calibrate the flexural resistance factor, ϕ , to achieve a preset target probability of failure.

RESEARCH SIGNIFICANCE

This paper proposes a strength reduction factor for use in flexural design of PSC bridge girders rehabilitated with CFRP laminates. The proposed factor is obtained via calibration of LRFD equations and is presented in a format that is suitable for adoption by code committees.

A limited parametric study shows that the proposed factor results in cross section designs that have an acceptable probability of failure for a broad range of design parameters.

FIBER SECTION METHOD

The analyses carried out in this study are performed using a computer program that makes use of the fiber section method. The program is designed to handle the construction sequence of PSC girders strengthened with CFRP and accounts for material non-linearity including concrete cracking, concrete crushing, steel yielding, and CFRP rupture. The developed program calculates the moment-curvature response of a given section and features a sophisticated graphical user interface that facilitates input and output data manipulation.

A fiber section analysis of the composite cross section entails discretization of the section into many layers (fibers) for which the constitutive models are based on uni-axial stress-strain relationships. Each region represents a fiber of material running longitudinally along the member and can be assigned one of several constitutive models representing the cast-in-place (CIP) deck concrete, pre-stressed girder concrete, CFRP laminates, reinforcing steel, and prestressing steel. The axial force and bending moment acting on the cross-section are evaluated as stress resultants through an iterative process that ensures compatibility and equilibrium within the cross-section. The iterative solution method used with the fiber section technique is documented elsewhere ⁵.

Constitutive Properties of Component Materials

The assumed constitutive material properties are illustrated in Fig. 1. Concrete fibers in compression are assumed to follow a nonlinear stress-strain relationship. In tension, concrete fibers crack after reaching the rupture strength, and after cracking, concrete resistance to

fades gradually to account for tension stiffening as shown in Figure 1-b. The brittle stress strain relationship assumed for **CFRP** is shown in Fig. 1-c. Pre-stressing strands are modeled assuming a Ramberg-Osgood function. The Ramberg-Osgood coefficients are taken as $a = 0.025$, $b = 118$, and $c = 10$ for low relaxation strands⁸. Additional details of the constitutive properties implemented in the model can be found in Ref. 5.

Accounting for the Construction Sequence

An equilibrium step is carried out at the time of transfer to calculate the initial camber-causing curvature using a two-stage iterative process that satisfies moment then force equilibrium within each increment. The technique implicitly accounts for the elastic shortening of the strands. All prestressing losses are assumed to occur at this stage and are accounted for in the calculations. After transfer and pre-stress loss calculations, the loading sequence associated with placement of non-monolithic decks is taken into account during the moment-curvature calculations using a process similar to that described below for CFRP laminates (Fig 2).

Rehabilitation of concrete structures using CFRP laminates usually takes place while the structure is subjected to a certain level of loading (taken equal to the full dead load in this study). Therefore, CFRP laminates are not strained while concrete and steel are both strained at the time of strengthening. The analysis method takes into account this situation as shown in Fig. 2. Just prior to strengthening the cross section with CFRP laminates, the cross section is subjected to a threshold moment $M_{i,,}$, resulting in the corresponding strain gradient shown in Fig. 2(c). Knowing that CFRP strains must be zero at this stage, and that subsequently applied moments (beyond $M_{i,,}$) will not result in identical strains in adjacent CFRP and concrete fibers, strains in CFRP fiber i are adjusted using the following equation:

$$\varepsilon_{CFRP,i} = \varepsilon_i - \varepsilon_{in,i}^{CFRP}$$

(1)

As shown in Figure 2(d), ε_i is the strain in the CFRP fibers corresponding to a moment higher than M_{in} and calculated assuming that the strain in adjacent concrete and CFRP fibers is identical. $\varepsilon_{in,i}^{CFRP}$ are the strains in concrete fibers adjacent to CFRP fibers at the threshold M_{in} moment. $\varepsilon_{CFRP,i}$ are the adjusted CFRP strains for a moment greater than M_{in} .

General Moment-Curvature Response

Figure 3 shows a moment-curvature ($M - \theta$) relationship that results from typical analyses of a PSC girder with and without bonded CFRP laminates. The relationship for the case with CFRP laminates shows key points of behavior such as at transfer, threshold moment points (point at which concrete deck is cast or CFRP is bonded), and ultimate point. After casting the CIP deck, the girder exhibits increased stiffness, which further increases when the CFRP is attached. Once the CFRP ruptures, the flexural strength of the cross-section drops sharply then gradually flattens out as the crack in the CFRP laminates travels up the web. The strengthened cross section does not fail completely, but exhibits a post-failure capacity equal to the strength of the original cross section.

Program Verification

The developed program has been extensively tested and verified by comparing analytical results to data obtained from experiments involving CFRP strengthened concrete girders. The ability of the program to predict the flexural behavior of *reinforced concrete* girders strengthened with CFRP is documented in Refs. 5 and 9. Figure 4 shows a comparison between

experimental and analytical $M - \theta$ curves for a T-shaped PSC girder. The experimental results are reported in Ref. 8. It is clear that the program captures all important aspects of behavior all the way up to failure.

The number of fibers into which a cross-section is discretized is taken as 60 in all analyses presented in this paper. This number was identified from convergence studies, which showed that employing more than 60 fibers to discretize reinforced concrete and PSC sections does not result in a significant improvement in accuracy ⁵.

DESIGN SPACE

Unstrengthened (Original) Bridges

Three simply supported bridges with varying spans are designed according to AASHTO-LRFD ⁷. These bridges form the core of the design space that is used as a basis for the reliability calculations. All bridges share the same road cross section shown in Fig. 5 (road width = 14180mm, slab thickness = 205mm, number of girders = 6, and girder spacing = 2440mm), but have different span lengths (18290mm, 24380mm, and 30480mm). The bridges are designated PS 18, PS24, and PS30, with the numbers corresponding to the nominal span length in meters. The concrete deck is assumed to be a cast-in-place (CIP) slab acting compositely with the girders.

Following the provisions of AASHTO-LRFD ⁷, each of the bridges is first designed to resist the applied dead and live loads. Only interior girders are designed, and since all bridges have simple spans, only positive moments are accounted for. The precast pre-stressed AASHTO girder is assumed to resist the dead loads (self-weight of girders and slab), while the composite section

(AASHTO girder and CIP slab) is assumed to resist live loads and additional dead loads (wearing surface and parapet load). Forces due to live loads are computed by superimposing the effect of a uniformly distributed lane load and the effect a standard truck or a tandem load whichever is greater (see Fig. 6). The truck/tandem portion of the live load moments are increased by an impact factor (IM) of 33% for the strength limit state and 15% for the fatigue limit state. When computing bending moments due to the standard truck for the strength limit state, the axle configuration used is based on a rear axle distance of 4300mm (AASHTO minimum value). For fatigue calculations, a similar configuration is used, however, the rear axle distance is taken as 9000mm. Table 1 summarizes the bending moments computed for the design of an interior girder of each bridge. The table also lists the distribution factor (DF) for the cases of one-lane (used for fatigue limit state) and two-lane loading (used for service and strength limit states).

Flexural design of the cross section is performed using the previously described fiber section program. The following material properties are assumed: compressive strength of CIP deck concrete = 27.6MPa, compressive strength of precast AASHTO girders = 48.3MPa, prestressing strands ultimate stress = 1860MPa for 12.5 mm diameter 7-wire low relaxation strands. Details of the designed cross section are shown in Fig. 7. A summary of the design stresses at transfer and at different service levels is given in Table 2. It is noteworthy that the flexural capacity of the designed cross sections is more than needed (compare the last columns in Tables 1 and 2) because serviceability conditions control the design (top cracking of girder at transfer, bottom cracking of girder at service, fatigue stress limit, ...etc.). This observation directly impacts the strengthening scheme described next.

Strengthened Bridges

To complete the design space, each girder designed above is assumed to have suffered some damage through the loss of a variable number of prestressing strands. The damaged girders are then strengthened to meet AASHTO LRFD ⁷ standards through CFRP rehabilitation. For each unstrengthened girder in the core design space, three levels of damage are considered, D1, D2, and D3, which correspond to nominal strand losses of around 10, 20, and 30% respectively. A beam that suffered a damage level of D 1 and then is strengthened using CFRP is designated as such by appending D1 to the naming system described above, e.g. PS18-D1. The three unstrengthened beams along with the nine strengthened beams (three strengthened designs for each original design) form a pool of bridge designs that account for design parameters of interest in this study. The developed pool of 12 designs forms the basis of the reliability calibration.

The damage scenario considered in this research is representative of a feasible situation that can occur over the life of a girder where strands are lost to corrosion, vandalism, or impact between over height vehicles and girders. As a result of the assumed damage the affected girders may or may not violate strength requirements. However, the girders no longer satisfy code provisions pertaining to service limit state stresses and are therefore in need of repair. The three levels of damage investigated are carefully chosen to represent realistic situations where repairing a damaged beam is more economical than replacing it.

Rehabilitation is achieved through the use of externally bonded CFRP laminates that are wrapped around the stem of the beams. This technique has been shown to be effective by several investigators including Ref. 4. Since the repair method does not involve additional prestressing, the service stress levels specified by AASHTO can no longer be satisfied. These stress limits are

imposed to insure that PSC girders do not have significant service cracks in the tension region, which can promote strand corrosion, and are therefore of no consequence since the bonded CFRP laminates cover up any existing cracks and will achieve this objective indirectly.

It is assumed that the CFRP laminates have 0.23 yarns/mm (6 yarns/inch) in the longitudinal direction and 0.19 yarns/mm (5 yarns/inch) in the transverse direction, and each yarn consists of 12000 fibers. This laminate configuration is one of the configurations successfully used by the Florida Department of Transportation (FDOT) for repair purposes. The manufacturer-provided tensile strength of the CFRP fibers is $\sigma_{\text{fiber}}=3.65\text{GPa}$ (530ksi). However, the usable tensile strength of the CFRP laminate is determined based on the Weibull Theory following an approach previously developed by the authors and described in Ref. 9. The developed theory accounts for size and stress gradient effects and the results are shown in Table 3 for the different girder designs. It can be seen that CFRP strength varies slightly with the level of damage for each bridge. This is because the required CFRP quantity becomes larger as the damage level increases, which results in a slightly reduced usable tensile strength according to the theory ⁹.

As a result of being proportioned to satisfy service stresses, the bridges with the lowest level of damage (PS18-D1, PS24-D1, and PS30-D1) have sufficient remaining flexural capacity after strand loss to resist the applied factored loads. A minimum CFRP amount of one layer (with $t_{\text{CFRP}} = 0.0109\text{mm}$) was nevertheless provided. The second and third damage levels (D2 and D3) had a more significant deficiency in flexural capacity, and hence required more than one layer of CFRP laminates. Table 4 lists the ratio of the flexural capacity generated by CFRP to the flexural capacity provided by the remaining prestressing strands. This ratio is of importance for evaluation of results as will be seen later on in the paper. One of the other advantages of using

CFRP for strengthening PS girders is that the service stresses in prestressing strands drop. This is shown in Table 4 which lists the strand stress at *Service I* limit state ($M_{service I} = M_D + M_{L+IM}$) for both damaged and strengthened cross sections. For the third damage level, it can be seen that the strand stress drops by around 12% after strengthening. This is beneficial to the behavior of the PSC beams from the fatigue point of view⁵.

Figure 8 shows the moment curvature relationships for Bridge PS30. Each graph corresponds to one of the three damage levels. Three $M - \theta$ relationships are included in each plot; the original $M - \theta$ for the undamaged section (bold line), $M - \theta$ for the damaged cross section before strengthening, and $M - \theta$ for the strengthened cross section after bonding the CFRP laminates. Also shown is the required capacity according to AASHTO-LRFD (horizontal line). The plots clearly show that adding CFRP to the system increases the flexural capacity of the cross section. This is however, accompanied by a substantial reduction in the ductility. The loss of ductility is accounted for in the calibration of the strength reduction factor.

RESISTANCE MODELS

Flexural resistance models are calculated by performing Monte Carlo simulations for the design space comprised of the original and strengthened cross sections. Five thousand data sets were randomly generated for each cross section, and therefore a total of sixty thousand cases were considered (4 cross sections [original + 3 strengthened] x 3 spans x 5000 data sets). Each data set varied randomly as a function of statistical models for the variables involved (bias [mean/nominal], coefficient of variation [COV = standard deviation/mean], and distribution type). The variables included in the study are dimensions, material properties, loads, and uncertainty of the analysis model. The statistical models used in this study were determined after

a review of the literature, which is summarized in Table 5. The table shows the values adopted in this study and values used by other researchers including ¹⁰⁻¹⁸. The current study assumes a normal distribution for all variables except for CFRP, which is assumed to be a Weibull material. The Weibull assumption results in a relatively low COV for the CFRP laminates, a fact that has been confirmed both analytically and experimentally ¹⁹.

Analyzing each of the data sets results in a unique $M - \theta$ relationship. Of interest in this study is the statistical variations in the ultimate moment strength (M_R). Analysis of data for the 5000 values of moment capacity for each design yielded the resistance models shown in Table 6. The table lists the nominal moment, M_n , obtained from a calculation based on the nominal value of the variables involved. Also listed in the table are the flexural resistance models, M_R , for each cross section based on the Monte Carlo simulations. Each resistance model is represented by mean value, bias, and COV. Sample histograms of the resistance models are illustrated in Fig. 9 for Bridge PS24. A Chi-squared goodness-of-fit study showed that all 12 distributions could be substituted with normal statistical distributions with good accuracy. Similar observations and assumptions were made by other researchers ¹³.

LRFD CALIBRATION

Probability of Failure and Reliability Index

The AASHTO LRFD ⁷ design code specifies a strength equation in the following format

$$\phi R \geq \sum \gamma_{Qi} Q_i \quad (2)$$

In Eq. 2, the resistance of the cross section, R , is scaled down by a reduction factor, ϕ , while the applied loads, Q_i , are scaled up by the load factors, γ_{Qi} . The values of ϕ and γ_{Qi} are determined through a calibration process that limits the probability of failure, P_f , to a small target value. The *Reliability Index*, β , is used to describe this probability of failure. The relationship between β and P_f is

$$P_f = \Phi(-\beta) \quad (3)$$

where $\Phi(\cdot)$ is a Cumulative Distribution Function (CDF) for a limit state function, Z , that represents the loading action in question; e.g. shear, flexure, ...etc. The simplest form of Z is

$$Z = R - Q \quad (4)$$

where, R , is the random resistance of the member and, Q , the random load effect acting on the member. In general, Z is more complex and involves a number of random variables, X_1, X_2, \dots, X_n , representing dimensions, material properties, loads ... etc.

First Order Reliability Method (FORM)

The reliability index, β , is calculated using FORM by finding the distance from the origin of the design space to the closest point (also known as the design point) on the limit state function (failure surface). The First Order Reliability Method (FORM) expands the limit state function using a first order Taylor series, which approximates the failure surface by a tangent plane at the point of interest. An iterative process executed on transformed standard normally distributed random vectors is employed to find the design point. A detailed description of this process can

be found in Ref. 20. A MatLab computer program was written to handle the iterative scheme in FORM and was used to determine the β values reported next.

β based on current AASHTO provisions (LRFD -1998)

The resistance models obtained previously were utilized to study the reliability of the designed cross sections. The use of resistance models simplifies the limit state function, which is especially helpful in reliability studies of highly nonlinear problems such as the one at hand. Equation 5 gives the limit state function used in the study.

$$Z = \alpha M_R (M_{WS} + M_D + \eta M_L) \quad (5)$$

In addition to uncertainties introduced by the load and resistance models (Tables 5 and 6), Z also accounts for uncertainty in the analysis model through the random variable, α , which is assumed to have a bias and COV of 1.01 and 4.5%, respectively^{12, 21}. The uncertainty in the girder distribution factor (which affects the live load moment calculations) is accounted for through the random variable, η , which has a bias and COV equal to 0.924 and 13.5%, respectively¹⁰. The uncertainties introduced by dynamic impact are treated following recommendations in Ref. 22 as follows. The static live load moment is increased by 10% to account for impact caused by two trucks for all lanes and a COV of the joint live and impact effect is taken as 18%. The live load is additionally increased by 5% to account for the heavy traffic volume assumed in this study (ADTT=5000 and 2 loaded lanes). The wearing surface moment (M_{ws}) was separated from dead load moments (M_D) to account for the different uncertainties associated with each variable (see Table 5).

The calculated twelve β values are given in Table 6 for the corresponding cross sections. The reliability index for the undamaged cross-sections is greater than 4.0, which significantly exceeds the AASHTO LRFD ⁷ target. This is expected since the design for these undamaged cross sections was controlled by limit states other than strength (cracking, fatigue, ...etc.). The strengthened cross sections had lower β values because strength was the controlling factor in the design process, which assumed that $\phi = 1.0$ according to AASHTO-LRFD ⁷. The listed values show that the current AASHTO design procedure is deficient when used for designing the PSC girders strengthened with CFRP laminates, i.e. results in cross sections with a reliability index below what is normally accepted.

An examination of Table 6 shows that β decreases with the increase of damage level up to D2, but climbs slightly for D3. This can be explained as follows. For the D 1 damage level, the cross-sections have greater strength than needed and hence the relatively high reliability index (compare Table 1 column 8 and Table 4 column 4). The reasons for this are: 1) the original sections are over strength to start with because serviceability checks controlled; 2) the assumed amount of damage was mild so that the damaged sections still satisfied strength provisions; and 3) a minimum of one layer of CFRP was added anyway to protect the damaged girders since serviceability stresses could not be satisfied. For the D2 damage level which violates strength provisions, just enough CFRP is added to reach the target strength using an unconservative $\phi = 1.0$ value, and so the reliability drops compared to D1. As the damage level increases to D3, more CFRP is needed for repair than for D2. Since the CFRP has a relatively low COV as discussed earlier, the reliability of the cross-section improves slightly as more CFRP is used, thereby increasing β . This is a desirable property of CFRP because the added brittleness introduced by the CFRP is somewhat tempered by improved reliability. The previous discussion

is valid for the failure mode observed in this study which was mostly controlled by CFRP rupture. Although other modes of failure may lead to other conclusions, it is unlikely for properly designed T-shaped bridge girders strengthened with CFRP laminates to fail by concrete crushing (due to the abundance of concrete in the deck) or steel rupture.

Calibration of the design procedure

The first step in calibrating the strength reduction factor is to establish a target value for β . Most modern design codes usually target a reliability index between 3.0 and 3.75. AASHTO-LRFD ⁷ maintains a target reliability index of 3.5. The reliability index takes into consideration factors such as the importance of the structure, the expected mode of failure, the ratio of live loads to dead loads, ...etc. ²³. In this study, it is assumed that the target reliability index for PSC girders with CFRP is $\beta_{PS-CFRP}^{target} = 3.75$. The adopted reliability index is greater than the 3.5 targeted by AASHTO to account for the brittle nature of CFRP rupture. As discussed previously, a CFRP-controlled mode of failure limits ductility considerably (see Fig. 8, for example). An increase of more than 0.25 is not warranted because the strengthened cross section does not fail completely, but exhibits a post-failure capacity equal to the strength of the damaged cross section (see Fig. 3). The reader is referred to Ref. 23 for a detailed discussion on the rationale behind choosing a target β .

To obtain cross sections with a reliability index equal to $\beta_{PS-CFRP}^{target}$, Eq. 2 needs to be calibrated. This can be done by either changing the reduction factor, ϕ , the load factors, γ_{Qi} , or both. In this study, calibration is performed by changing the reduction factor and not the load factors. The impact of changing ϕ on β is illustrated in Fig. 10-a for a wide range of $\phi = 0.75 - 1.0$.

The plot shows that low ϕ values result in overly conservative designs (P more than 4.5). A ϕ value of 1.0 (current AASHTO provision for flexural design of PSC girders) is clearly unconservative, especially for the second and third damage levels. To reach a ϕ value that results in cross-sections with β equal to 3.75 (target value), the plot in Fig. 10-b is used. The abscissa in this plot is the ϕ value and the ordinate is the square of the difference between the resulting β and $\beta_{PS-CFRP}^{target}$; i.e. $(\beta - \beta_{PS-CFRP}^{target})^2$. The lowest point on the curve corresponds to ϕ that would result in β closest to $\beta_{PS-CFRP}^{target}$ and is determined through nonlinear regression. The first nine values in Table 7 are the computed strength reduction factors obtained for the damaged cross sections. If the results for each damage level are considered together, a plot similar to the one in Fig. 10-b would be used, however, the ordinate would be the square of $(\beta - \beta_{PS-CFRP}^{target})^2$ from all cross sections. The resulting ϕ in this may be called an optimum since it results in the least differences between β and $\beta_{PS-CFRP}^{target}$ for a wider range of cross sections. A calibration of all the obtained data together shows a ϕ value of 0.91 is needed to design cross sections with β values of 3.75.

Proposed Resistance Factor, ϕ

A review of Table 7 shows that the choice of the lowest value of ϕ (say 0.85) for design may result in over conservative cross sections, especially for low damage levels. It is therefore proposed that a transition relationship for ϕ be used as shown in Fig. 11. The proposed reduction factor uses the ratio of cross-sectional capacity from CFRP laminates to the capacity from prestressing strands (M_{CFRP}/M_{PS}) as the controlling parameter. This ratio is believed to better represent the amount of CFRP laminates in the cross section than the actual area, which is

to be determined in a design situation, thus eliminating the need for unnecessary design cycles. The calibrated ϕ values for the 12 cross sections are plotted in Fig. 11 versus M_{CFRP}/M_{PS} . The undamaged cross sections are represented by the points on the ordinate axis; i.e. $M_{CFRP}/M_{PS} = 0.0$. The damaged cross sections are represented by the other nine points in the plot. The proposed reduction factor (dashed line) is a lower bound for the computed values, which is given by the following equation

$$\phi = 1.0 - \frac{M_{CFRP}}{M_{PS}} \geq 0.85 \quad (6)$$

The minimum limit of 0.85 is imposed on ϕ to follow the trend observed in this plot.

The effect of using the proposed ϕ for a wide range of dead load to live load ratios is given in Fig. 12 for Bridge PS 18. It can be seen that using the proposed equation for ϕ results in acceptable β values for a wide range of M_L/M_D . The difference between the four curves plotted in Fig. 12 is small since the proposed the ϕ proposed in Eq. 6 is used in the calculations.

SUMMARY AND CONCLUSIONS

The flexural reliability of PSC bridge girders strengthened with CFRP laminates is investigated. A detailed nonlinear analysis model that accounts for material nonlinearities and construction sequence is developed. Monte Carlo simulations are performed using the developed model to determine resistance models for a limited number of PSC girder cross sections strengthened with CFRP. The developed resistance models are then used to calibrate the AASHTO-LRFD strength provisions using the first order reliability method. It is proposed that the strength reduction factor, ϕ , follow Eq. 6, which is shown to result in acceptable reliability

for a wide range of dead load to live load ratios. Since Equation 6 was calibrated using a limited design space, further studies are needed to confirm that it works well for a wider range of parameters. This study focused solely on flexural behavior of cross-sections strengthened with CFRP. Further research is needed to investigate the probabilistic nature of other modes of failure including shear resistance of beams strengthened with CFRP laminates as well as peel-off and debonding of laminates.

ACKNOWLEDGEMENTS

This paper is based on research supported in part by the Florida Department of Transportation (Contract BC-190) and the Department of Civil and Environmental Engineering at the University of Central Florida. The authors would also like to acknowledge the support and contributions of Dr. Mohsen Shahawy and Mr. Thomas Beitelman to this research.

REFERENCES

1. ACI, *State-of-the-Art Report on Fiber Reinforced Plastic Reinforcement for Concrete Structures*, Report by ACI Committee 440, American Concrete Institute, Box 19150, Redford Station, Detroit, Michigan 48219, USA, 1996.
2. Triantafillou, T.C. and Pelvis, N. "*Strengthening of RC Beams with Epoxy-bonded Fibre-Composite Materials*", *Materials and Structures*, No. 25, 1992, pp. 201-211.
3. Arduini, M. and Nanni, A. "*Parametric Study of Beams with externally Bonded FRP Reinforcement*", *Structural Journal*, ACI, Vol. 94, No. 5, 1997, pp. 493-501.
4. Shahawy, M., and Beitelman T.E. "*Static and Fatigue Performance of RC Beams Strengthened with CFRP Laminates*", *Journal of Structural Engineering*, ASCE, Vol. 125, No. 6, 1999, pp. 613-621.

5. El-Tawil, S., Ogunc, C., Okeil, A.M., and Shahawy, M. *"Static and Fatigue Analyses of RC Beams Strengthened with CFRP Laminates,"* Journal of Composites for Construction, ASCE, 2001. (accepted for publication)
6. Bakht, B., Al-Bazi, G., Banthia, N., Cheung, M., Erki, M-A., Faoro, M., Machida, A., Mufti, A.A., Neale, K.W., and Tadros, G. *"Canadian Bridge Design Code Provisions For FiberReinforced Structures,"* Journal of Composites for Construction, AS CE, Vol. 4, No. 1, 2001, pp. 3-15.
7. AASHTO, *LRFD Bridge Design Specifications*, American Association of State Highway and Transportation Officials, Washington, D.C., 1998.
8. Collins, M. P. and Mitchell, D., *Prestressed Concrete Structures*, Prentice Hall, Inc., New Jersey, USA, 1991.
9. Okeil, A.M., El-Tawil, S., and Shahawy, M. *"Short-Term Tensile Strength Of CFRP Laminates For Flexural Strengthening Of Concrete Girders,"* Structural Journal, ACI, Vol. 98, No. 4, 2001, (in press).
10. Kennedy, D.J.L., Gagnon, D.P., Allen, D.E., and MacGregor, J.G). *"Canadian Highway Bridge Evaluation: Load and Resistance Factors,"* Canadian Journal of Civil Engineering, 19, 1992, pp. 992-1006.
11. Lu, R., Luo, Y. and Conte, J.P. *"Reliability Evaluation of Reinforced Concrete Beams,"* Structural Safety, El Sevier, Vol. 14, No. 4, 1994, pp. 277-298.
12. Nowak, A.S., Yamani, A.S., and Tabsh, S.W. *"Probabilistic Models for Resistance of Concrete Girders,"* Structural Journal, ACI, Vol. 91, No. 3, 1994, pp. 269-276.

13. Pelvris, N., Triantafillou, T.C., and Venesiano, D. *"Reliability of RC Members Strengthened with CFRP Laminates,"* Journal of Structural Engineering, ASCE, Vol. 121, No. 7, 1995, pp. 1037-1044.
14. Thoft-Christensen, P. *"Assessment of the Reliability Profiles for Concrete,"* Engineering Structures, El Sevier, Vol. 20, No. 11, 1998, pp. 1004-1009.
15. Val, D., Stewart M., and Melchers, R. *"Bridges Effect of Reinforcement Corrosion on Reliability of Highway Bridges,"* Engineering Structures, El Sevier, Vol. 20, No. 11, 1998, pp. 1010-1019.
16. Crespo-Minguillon, C. and Casas, J.R. *"Fatigue Reliability Analysis of Prestressed Concrete Bridges,"* J. of Structural Engineering, ASCE, Vol. 124, No. 12, 1999, pp. 1458-1466.
17. Estes, A. and Frangopol, D. *"Repair Optimization of Highway Bridges using System Reliability Approach,"* Journal of Structural Engineering, ASCE, Vol. 125, No. 7, 1999, pp. 766-775.
18. Stewart, M., and Val, D. *"The Role of Load History in Reliability-Based Decision Analysis of Aging Bridges,"* Journal of Structural Engineering, ASCE, Vol. 125, No. 7, 1999, pp. 776-783.
19. Bullock, R.E. *"Strength Ratios of Composite Materials in Flexure and in Tension,"* Journal of Composite Materials, No. 8, 1974, pp. 200-206.
20. Estes, A. and Frangopol, D. *"RELSYS: A computer program for Structural System Reliability,"* Structural Engineering and Mechanics, Vol. 6, No. 8, 1998, pp. 901-919.
21. Ellingwood, B. Galambos, T., MacGregor, J., and Cornell, A., *Development of a Probability Based Load Criterion for American National Standard A58: building code requirements for*

minimum design loads in buildings and other structures, National Bureau of Standards, SP 577, Washington, USA, 1980.

22. Nowak, A.S. and Collins, K.R., *Reliability of Structures*, , McGraw Hill Higher Education Division, McGraw Hill, USA, 2000.
23. Allen, D.E. "*Canadian Highway Bridge Evaluation: Reliability Index*, " Canadian Journal of Civil Engineering. 19. 1992. pp. 593-602.

LIST OF NOTATIONS

a, b, c	Ramberg-Osgood coefficients for strand stress-strain relationship
f'_c	concrete compressive strength
f_{pu}	strand ultimate stress.
M_{in}	threshold moment (initial moment acting at time of CFRP application)
M_R	actual flexural capacity of beam
M_D	moment due to dead load
M_{WS}	moment due to weight of wearing surface
M_L	moment due to live loads (lane + (truck or tandem))
M_{CFRP}	flexural capacity from CFRP laminates
M_{PS}	flexural capacity from CFRP laminates
M_n	nominal flexural capacity of beam
P_f	probability of failure of a composite fiber
Q_i	applied loads
R	structural resistance
t_{CFRP}	thickness of CFRP laminate
Z	limit state (performance) function

α	model uncertainty
β	<i>Reliability Index</i>
$\beta_{PS-CFRP}^{target}$	target reliability index for PSC girders strengthened with CFRP laminates
γ_{Qi}	load factors
ϵ_i	strain in concrete adjacent to CFRP fiber i at M
$\epsilon_{in,i}^{CFRP}$	strain in concrete adjacent to CFRP fiber i at M_{in}
$\epsilon_{CFRP,i}$	adjusted strain in CFRP fiber i at M
$\Phi(\cdot)$	Cummulative Distribution Function (CDF)
ϕ	reduction factor
η	uncertainty in girder distribution factor
σ_{fiber}	tensile strength of a single CFRP fiber (as reported by manufacturer)
σ_{beam}	short-term tensile strength of a CFRP laminate wrapped around the stem of a beam
θ	curvature of cross section due to flexure
COV	coefficient of variation

LIST OF TABLES:

Table 1: Design moments for interior girder of reinforced concrete bridges 26

Table 2: Summary of design stresses and capacities.....27

Table 3: Usable tensile stress used in design of PS Bridges 28

Table 4: Design summary of bridge cross sections.....29

Table 5: Statistical properties of variables involved in the study 30

Table 6: Results of Monte Carlo simulation (moment units in kN.m) 31

Table 7: Optimum θ to achieve $\beta_{PS-CFRP}^{target}$ 32

Table 1: Design moments for interior girder of reinforced concrete bridges.

Bridge	Distribution Factor		Service Moments (kN.m)				Factored Moment
	1 Lane	2 Lanes	Dead Load	Service III	Service I	Fatigue	M_u (kN.m)
PS 18	0.4927	0.6735	727	1900	2151	346	3358
PS24	0.4749	0.6657	1509	3301	3674	531	5600
PS30	0.4676	0.6684	2762	5298	5814	719	8678

Table 2: Summary of design stresses and capacities.

Bridge	Cross Section			Concrete Stresses (MPa)					Fatigue Strand Stresses Δf_{PS} (MPa)	Flexural Capacity M_n (kN.m)
	Deck thickness (mm)	Girder Type	Number of Strands	Transfer f_{tgi}	Ser. III f_{bgi}	Service I F_{bg}	f_{tg}	f_{td}		
PS 18	205	II	26	-1.80	-21.57	+3.37	-16.74	-4.71	15.86	4050
PS24	205	III	34	-0.76	-19.66	+3.28	-15.94	-4.94	15.35	6756
PS30	205	IV	44	-1.58	-17.70	+3.50	-16.55	-5.12	13.92	10520

Table 3: Usable tensile stress used in design of PS Bridges

Bridge Case	Damage		σ_{beam} GPa
	Strands	A_{ps} (%)	
PS 18-D1	3	11.54	1.97
PS 18-D2	6	23.08	1.95
PS 18-D3	9	34.62	1.92
PS24-D1	4	11.76	1.99
PS24-D2	8	23.53	1.96
PS24-D3	12	35.29	1.94
PS 30-D1	5	11.36	1.97
PS30-D2	10	22.72	1.95
PS30-D3	15	34.09	1.92

Table 4: Design summary of bridge cross sections

Bridge	CFRP	Flexural Capacity		$\frac{M_{CFRP}}{M_{PS}}$	Strand Stress at Service I		
	thickness	(kN.m)			Damaged	Strengthened	Diff.
	t_{CFRP}	Damaged	Strengthened		(GPa)	(GPa)	(%)
	(mm)						
PS 18	--		4050	--		1.13	-
PS 18-D1	0.109*	3557	3683	0.0827	1.22	1.17	3.5
PS 18-D2	0.179	3059	3357	0.1579	1.39	1.27	8.4
PS 18-D3	0.381	2584	3358	0.4015	1.59	1.41	11.2
PS24	--		6756	--		1.12	-
PS24-D1	0.109*	5971	6095	0.0713	1.19	1.16	2.2
PS24-D2	0.198	5175	5606	0.1496	1.40	1.27	9.0
PS24-D3	0.430	4386	5607	0.3837	1.59	1.40	12.0
PS30	--		10520	--		1.12	-
PS30-D1	0.109*	9374	9495	0.0614	1.17	1.15	1.5
PS30-D2	0.184	8220	8678	0.1192	1.35	1.24	8.3
PS30-D3	0.433	7078	8677	0.3250	1.54	1.36	11.7

* a minimum thickness is used equal to thickness of one

Table 5: Statistical properties of variables involved in the study

Variable	Other Researchers			Current Study		
	Bias	COV (%)	Distribution Type	Bias	COV (%)	Distribution Type
Dimensions (h, d, b)	1.00 - 1.03	0.5 - 7.0	Normal	1.00	3.0	Normal
Area of steel (\sim)	1.00	0.0-4.0	Normal -	1.00	1.5	Normal
Concrete strength ($f\sim$)	0.81 - 1.25	9.0 - 21.0	Deterministic Normal -	1.10	18.0	Normal
Strand strength (f_{pu})	1.00 - 1.04	1.7 -2.5	LogNormal Normal -	1.04	2,0	Normal
CFRP failure Analytical	1.33	7.4-10.0	Weibull	1.10	2.2	Weibull
strain ($\epsilon_{u,CFRP}$)* Experimental	--	2.2-5.1	--	--	-	
CFRP						
Model Uncertainty (α)	1.01-1.10	4.5-12.0	Normal	1.01	4.5	Normal
Uncertainty of Girder DF (η)	0.89-1.02	9.1-14.0	Normal	0.924	13.5	Normal
Wearing Surface Load (WS)	1.00-1.44	8.0-53.2	Normal	1.10	20.0	Normal
Dead Load (D,)	1.00-1.05	8.2-25.0	Normal	1.05	10.0	Normal
Buildings	1.20	9.0-25.0	Extreme Event I	--	--	-
Live Load (L)						
Bridges	1.25-1.52	12.0-41.0	Normal - Modified Normal	1.35-	18.0	Normal

* analytical results used by Pelvris et al. (1995); experimental results are reported in Bakht et al. (2000).

Table 6: Results of Monte Carlo simulation (moment units in kN.m)

Case	M_L/M_D	M_n	M_R			Reliability Index
			Value	Bias	COV	β
PS18		4050	4232	1.045	2.84	3.93
PS18-D1		3683	3892	1.057	2.37	3.34
PS18-D2	1.40	3357	3559	1.060	2.26	2.70
PS18-D3		3358	3589	1.069	2.08	2.77
PS24		6756	7055	1.044	2.89	4.03
PS24-D1		6095	6436	1.056	2.36	3.35
PS24-D2	1.04	5606	5942	1.060	2.25	2.74
PS24-D3		5607	5988	1.068	2.12	2.81
PS30		10520	10980	1.044	2.87	4.24
PS30-D1		9495	10020	1.055	2.42	3.52
PS30-D2	0.80	8678	9180	1.058	2.28	2.81
PS30-D3		8677	9253	1.066	2.13	2.88

Table 7: Optimum ϕ to achieve $\beta_{PS-CFRP}^{target}$

Case		Optimum ϕ
	D1	0.936
PS18	D2	0.875
	D3	0.884
	D1	0.939
PS24	D2	0.887
	D3	0.893
	D1	0.954
PS30	D2	0.899
	D3	0.905
All D1	cases	0.944
All D2 cases		0.888
All D3 cases		0.895
All cases		0.910

LIST OF FIGURES:

Figure 1: Monotonic constitutive models for component materials 34

Figure 2: Sequence of analysis for girders with CFRP-strengthened girders with composite decks..... 35

Figure 3: Idealized moment-curvature relationships for PSC girders strengthened with CFRP laminates..... 36

Figure 4: Experimental vs. analytical $M - \phi$ relationship for verification. 37

Figure 5: Cross section of 6-girder bridge 38

Figure 6: Loading cases considered in design of bridges.....39

Figure 7: Cross sections of undamaged interior bridge girders.40

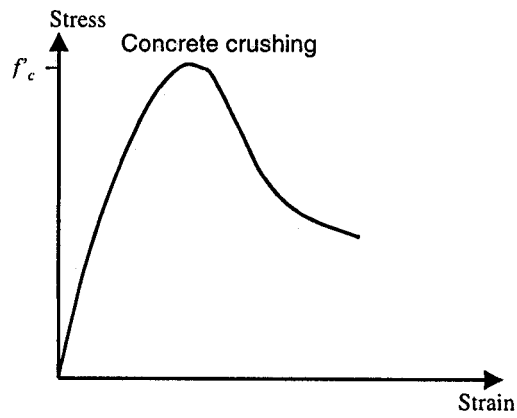
Figure 8: Moment - curvature relationships for interior girder (PS30)41

Figure 9: Histograms of flexural resistance for Bridges PS24, PS24-D1, PS24-D2, and PS24-D3. 42

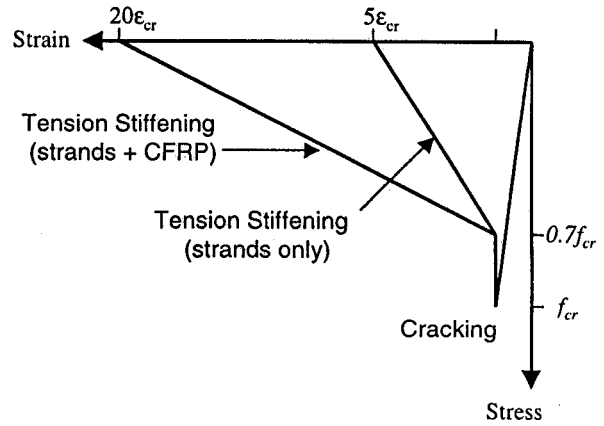
Figure 10: (a) effect of changing ϕ on the β , (b) determining the optimum reduction factor, ϕ . (Bridges PS24-D1, PS24-D2, and PS24-D3)..... 43

Figure 11: Proposed reduction factor, ϕ 44

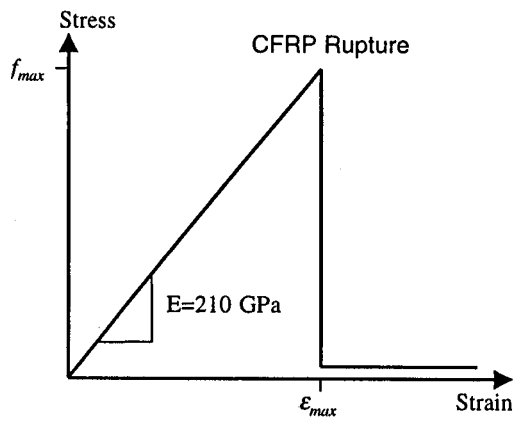
Figure 12: Effect of M_L/M_D on Reliability Index, β . (Bridge PS18, proposed ϕ).....45



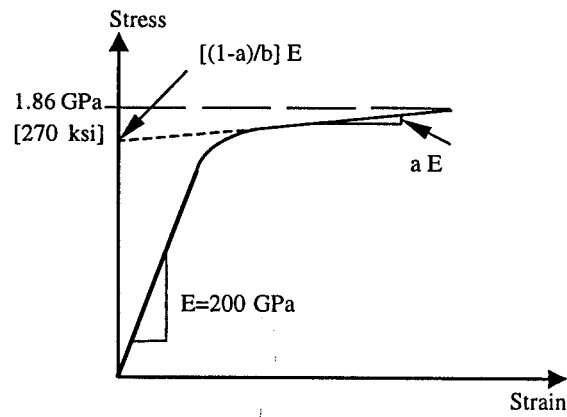
(a) Concrete in compression



(b) Concrete in tension



(c) CFRP in tension



(d) Prestressing strands

Figure 1: Monotonic constitutive models for component materials

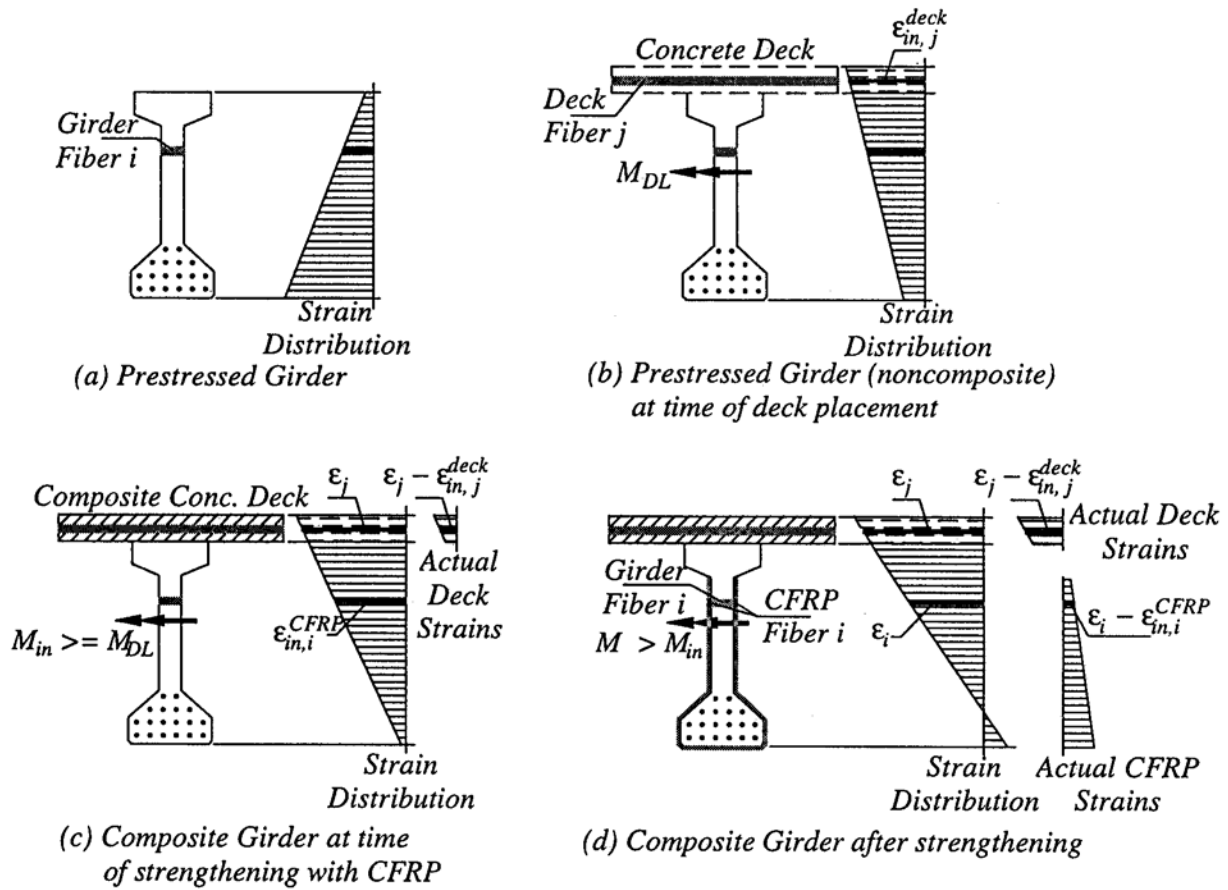


Figure 2: Sequence of analysis for girders with CFRP-strengthened girders with composite decks.

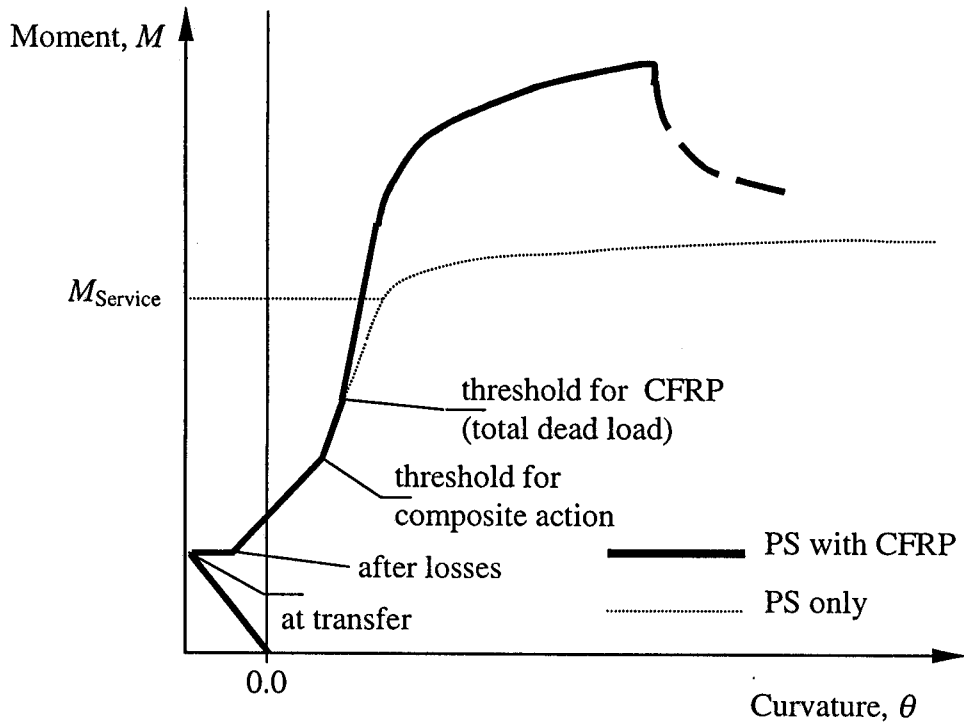


Figure 3: Idealized moment-curvature relationships for PSC girders strengthened with CFRP laminates.

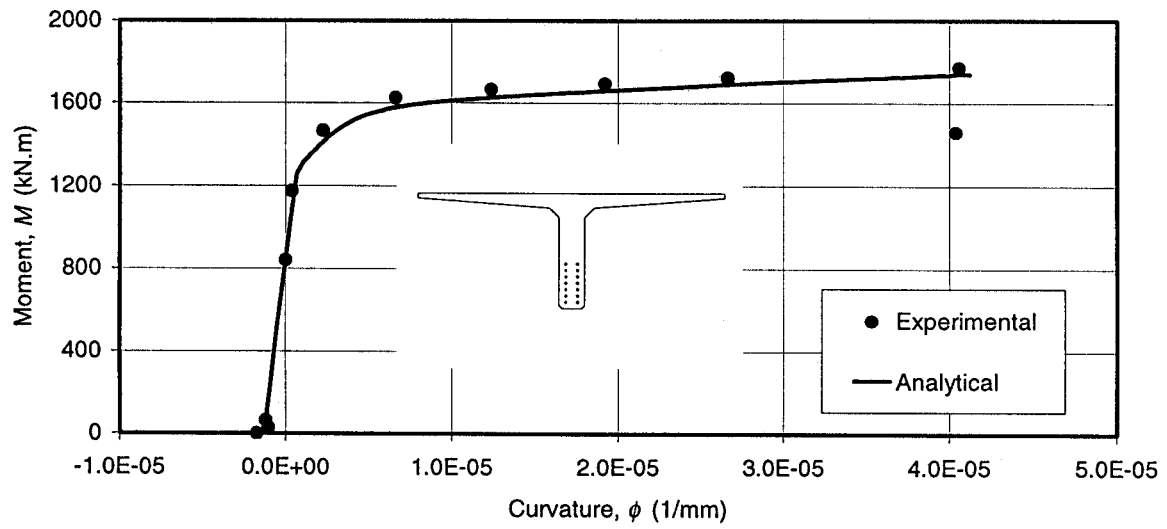


Figure 4: Experimental vs. analytical $M - \theta$ relationship for verification.

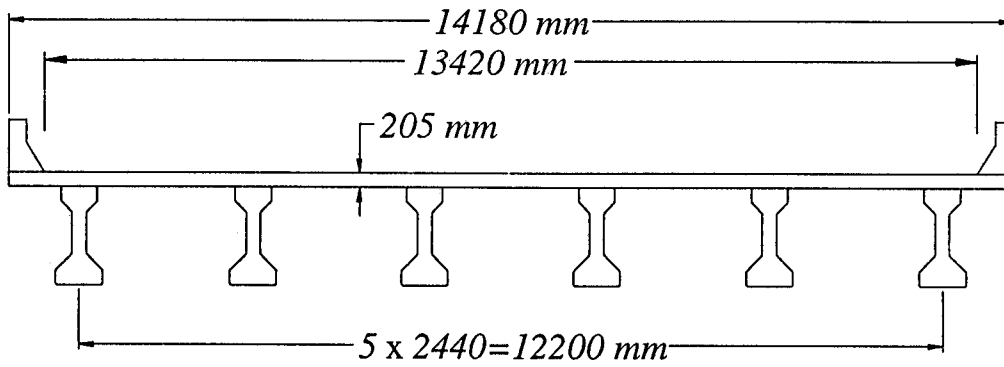


Figure 5: Cross section of 6-girder bridge

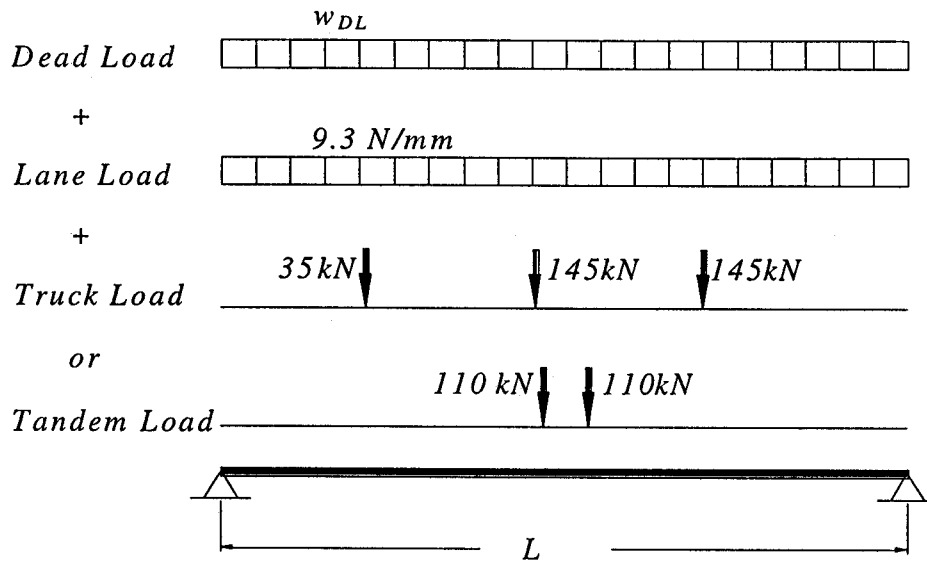


Figure 6: Loading cases considered in design of bridges

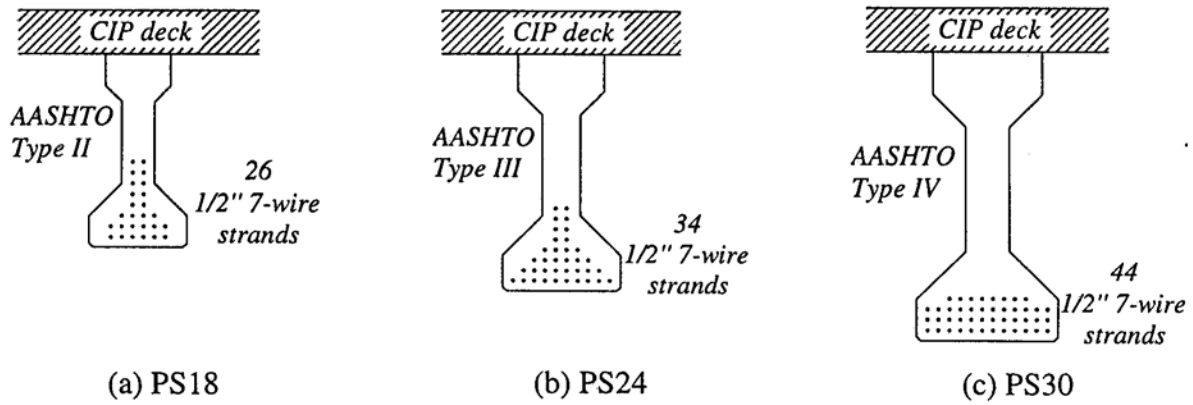
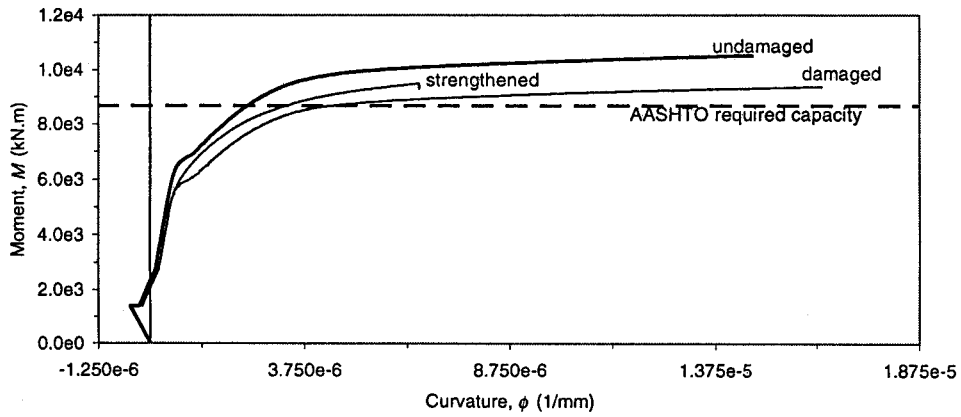
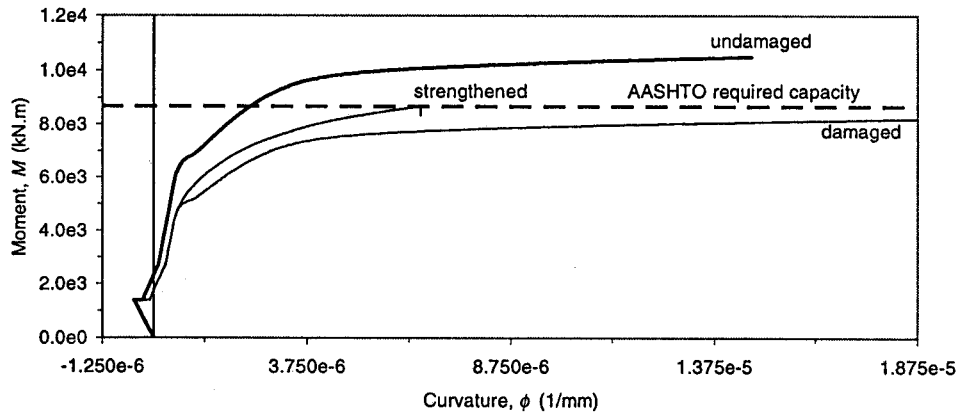


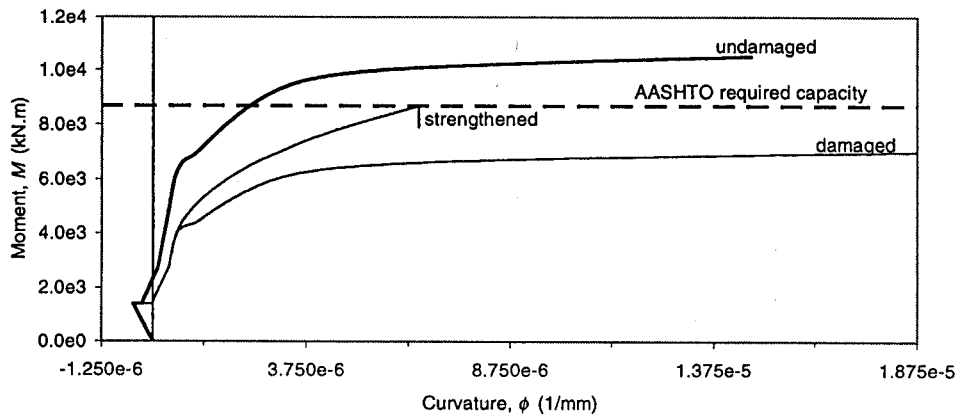
Figure 7: Cross sections of undamaged interior bridge girders.



(a) 1st damage level (PS30-D1)

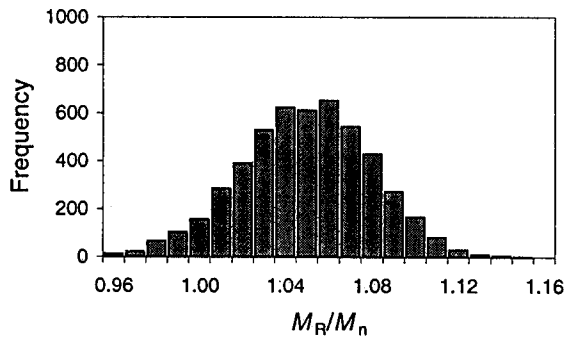


(b) 2nd damage level (PS30-D2)

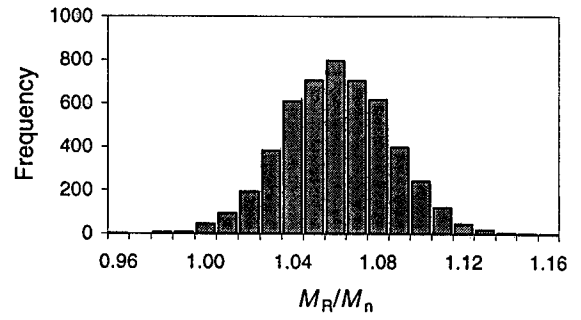


(c) 3rd damage level (PS30-D3)

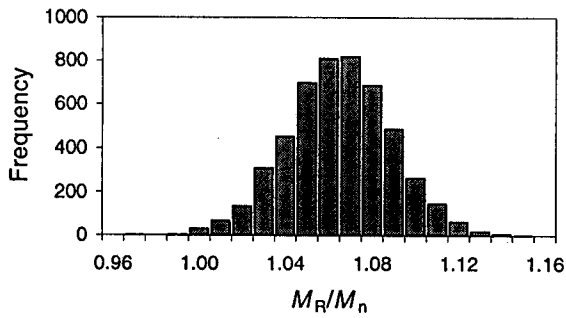
Figure 8: Moment - curvature relationships for interior girder (PS30)



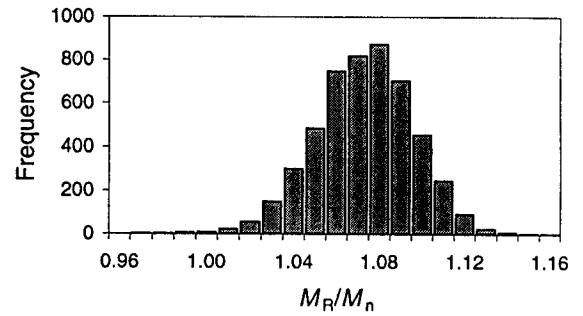
(a) PS24



(b) PS24-D1

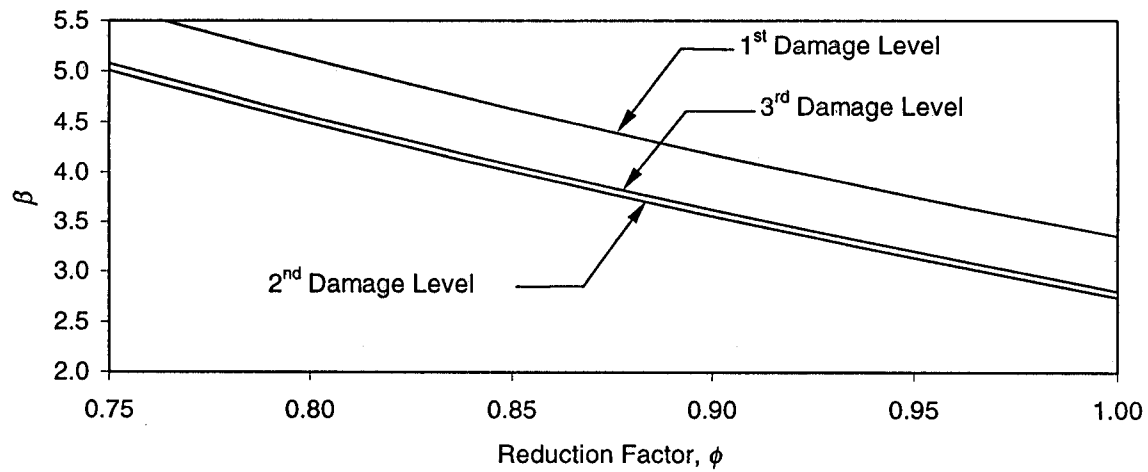


(c) PS24-D2

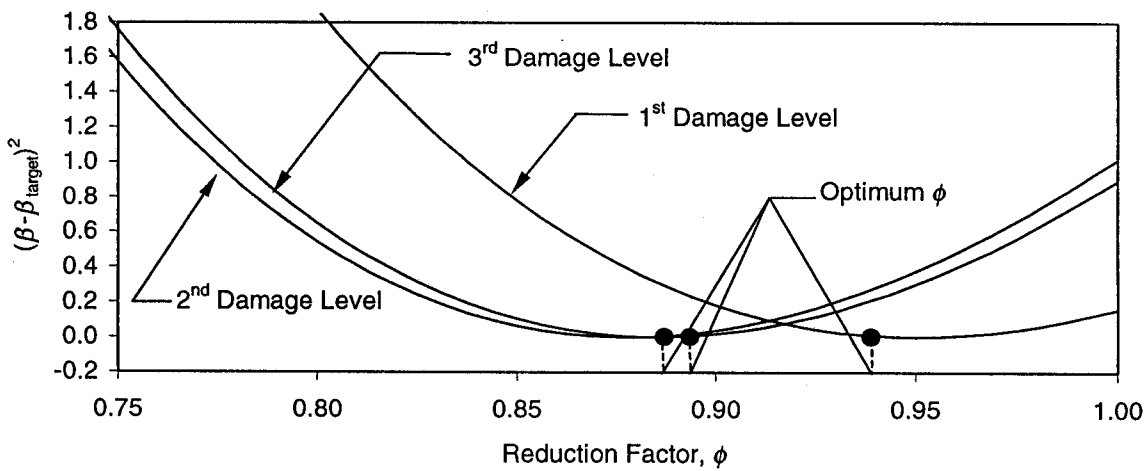


(d) PS24-D3

Figure 9: Histograms of flexural resistance for Bridges PS24, PS24-D1, PS24-D2, and PS24-D3.



(a)



(b)

Figure 10: (a) effect of changing ϕ on the β , (b) determining the optimum reduction factor, ϕ . (Bridges PS24-D1, PS24-D2, and PS24-D3)

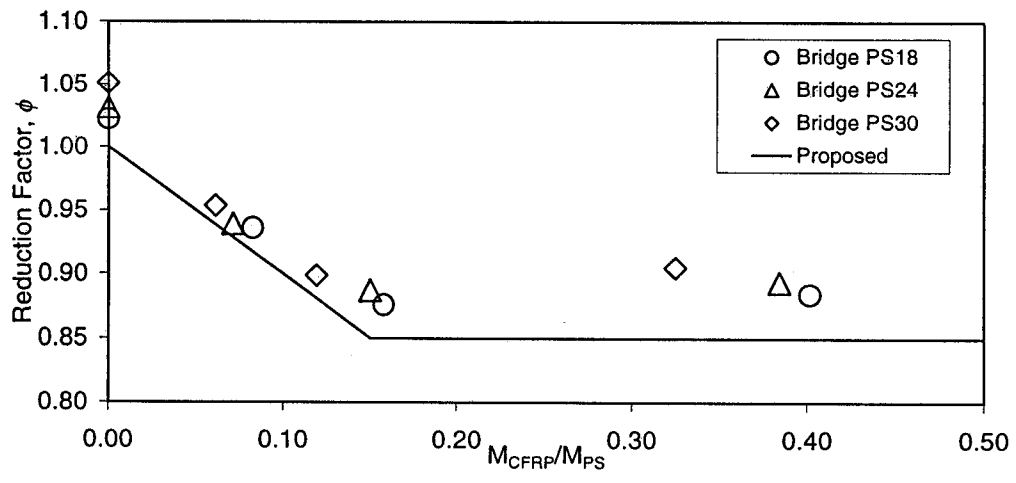


Figure 11: Proposed reduction factor, ϕ .

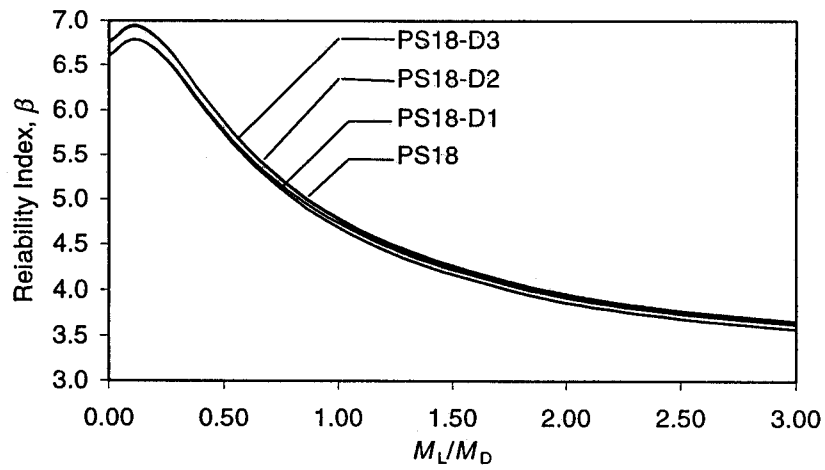


Figure 12: Effect of M_L/M_D on Reliability Index, β . (Bridge PS18, proposed ϕ)